Journal of Environmental Management xxx (xxxx) 112462

Contents lists available at ScienceDirect

Journal of Environmental Management

journal homepage: www.elsevier.com/locate/jenvman

# Vegetation structure parameters determine high burn severity likelihood in different ecosystem types: A case study in a burned Mediterranean landscape

José Manuel Fernández-Guisuraga [a, *], Susana Suárez-Seoane [b], Paula García-Llamas [a], Leonor Calvo [a]

[a] Area of Ecology, Faculty of Biological and Environmental Sciences, University of León, 24071, León, Spain
[b] Department of Organisms and Systems Biology (BOS, Ecology Unit) and Research Unit of Biodiversity (UMIB; UO-CSIC-PA), University of Oviedo, Oviedo, Mieres, Spain

ARTICLE INFO

*Keywords:*
Albedo
Burn severity
LiDAR
Pre-fire management
Sentinel-2
Vegetation structure

ABSTRACT

The design and implementation of pre-fire management strategies in heterogeneous landscapes requires the identification of the ecological conditions contributing to the most adverse effects of wildfires. This study evaluates which features of pre-fire vegetation structure, estimated through broadband land surface albedo and Light Detection and Ranging (LiDAR) data fusion, promote high wildfire damage across several fire-prone ecosystems dominated by either shrub (gorse, heath and broom) or tree species (Pyrenean oak and Scots pine). Topography features were also considered since they can assist in the identification of priority areas where vegetation structure needs to be managed. The case study was conducted within the scar of a mixed-severity wildfire that occurred in the Western Mediterranean Basin. Burn severity was estimated using the differenced Normalized Burn Ratio index computed from Sentinel-2 multispectral instrument (MSI) Level 2 A at 10 m of spatial resolution and validated in the field using the Composite Burn Index (CBI). Ordinal regression models were implemented to evaluate high burn severity outcome based on three groups of predictors: topography, pre-fire broadband land surface albedo computed from Sentinel-2 and pre-fire LiDAR metrics. Models were validated both by 10-fold cross-validation and external validation. High burn severity was largely ecosystem-dependent. In oak and pine forest ecosystems, severe damage was promoted by a high canopy volume (model accuracy = 79%) and a low canopy base height (accuracy = 82%), respectively. Land surface albedo, which is directly related to aboveground biomass and vegetation cover, outperformed LiDAR metrics to predict high burn severity in ecosystems with sparse vegetation. This is the case of gorse and broom shrub ecosystems (accuracy of 80% and 77%, respectively). The effect of topography was overwhelmed by that of the vegetation structure portion of the fire triangle behavior, except for heathlands, in which warm and steep slopes played a key role in high burn severity outcome together with horizontal and vertical fuel continuity (accuracy = 71%). The findings of this study support the fusion of LiDAR and satellite albedo data to assist forest managers in the development of ecosystem-specific management actions aimed at reducing wildfire damage and promote ecosystem resilience.

**List of acronyms**

| | |
|---|---|
| bLSA | broadband Land Surface Albedo |
| CBI | Composite Burn Index |
| CNIG | Spanish National Center of Geographic Information |
| CSM | Canopy Surface Model |
| CV | Coefficient of Variation |
| dNBR | difference of the Normalized Burn Ratio |
| DTM | Digital Terrain Model |
| ETM+ | Enhanced Thematic Mapper Plus |
| GPS | Global Positioning System |
| LiDAR | Light Detection and Ranging |
| ML | Maximum Likelihood |
| MSI | Multispectral Instrument |
| NIR | Near Infrared |
| PNOA | Spanish Aerial Ortho-photography National Planning |
| PO | Proportional Odds |

* Corresponding author.
*E-mail address:* jofeg@unileon.es (J.M. Fernández-Guisuraga).

https://doi.org/10.1016/j.jenvman.2021.112462
Received 22 October 2020; Received in revised form 10 March 2021; Accepted 19 March 2021

| | |
|---|---|
| SD | Standard Deviation |
| SWIR | Short-Wave Infrared |
| TM | Thematic Mapper |

## 1. Introduction

Fire is a major ecological disturbance in forest and shrub ecosystems worldwide (Bennett et al., 2016; Bassett et al., 2017), affecting not only vegetation structure and composition (Pausas and Keeley, 2009), wildlife habitat (Dunn and Bailey, 2016) and ecosystem services provisioning (Robinne et al., 2020), but also ecosystem biogeochemical cycles (Lasslop et al., 2019) and land surface energy budgets, leading to a forcing on the regional to global climate (Ward et al., 2012; Archibald et al., 2018). Burn severity, quantified by the change in aboveground and belowground organic matter (Keeley, 2009), is one of the most critical factors influencing long-term ecological effects of fire (Harris and Taylor, 2017). In the Mediterranean Basin, forest surface burned at high severity is expected to increase due to climate change (Niccoli et al., 2019), land use changes (Chuvieco et al., 2010) and a lack of adequate forest management practices for enhancing long-term adaptation to global change (Vilà-Cabrera et al., 2018). In most cases, burn severity can exhibit a large spatial variability within single fire events (mixed-severity wildfires), particularly with increasing landscape heterogeneity (Alexander et al., 2006; Viedma et al., 2020). Patterns of burn severity in heterogeneous wildfires are mainly controlled by three major drivers: topography, weather and vegetation (Alexander et al., 2006; Oliveras et al., 2009; Viedma et al., 2015; Fang et al., 2018). However, the role of these drivers and their complex interactions is not always clear (Lecina-Diaz et al., 2014; Parks et al., 2018).

Topography strongly influences local weather conditions (Mitsopoulos et al., 2019), vegetation composition and structure (Lydersen and North, 2012), as well as fire behavior (Harris and Taylor, 2017). However, contradictory topographic effects on burn severity have been reported. Several studies found a strong relationship between burn severity and topography even under extreme weather conditions (Broncano and Retana, 2004; Viedma et al., 2015; Harris and Taylor, 2017). Conversely, other studies have suggested either the absence of a clear effect of topography on burn severity (Turner et al., 1999) or the overwhelming of their effects by fuel structure or fire weather (Zald and Dunn, 2018; García-Llamas et al., 2019a). Among fire weather variables, temperature, relative humidity and wind have proven to be strong drivers of fire behavior and burn severity (Dillon et al., 2011; Estes et al., 2017; García-Llamas et al., 2019a), as they control fire spread rate and fuel moisture content (Plucinski, 2003). However, the lack of meteorological data at high spatial and temporal resolution restricts the use of weather variables for explaining the spatial variation of burn severity at fine spatial scales (Fang et al., 2018; Viedma et al. 2015, 2020). Fuel characteristics, mainly ecosystem dominant species and vegetation structure, are usually reported to strongly influence fire spread and burn severity (Coppoletta et al., 2016; García-Llamas et al., 2019a), sometimes regardless of topography and fire weather conditions (Harris and Taylor, 2017). For example, in the western Mediterranean Basin, Fernandes et al. (2010) found that fire spread rate and burn severity decreased from a maritime pine (*Pinus pinaster* Aiton) stand to contiguous stands of short-needled conifers and deciduous broadleaved forest. The same behavior was observed by Thompson and Spies (2009) in a Mediterranean mixed-forest of North America. Also, they found that increased surface fuel loadings were related to high conifer crown damage. For its part, Safford et al. (2009) stated that fuel loadings were more important than topography in driving burn severity under Mediterranean climate in Sierra Nevada, United States. Conversely, fire weather conditions, rather than vegetation composition and structure, appear to exert the largest influence on burn severity in subalpine forests across the Rocky Mountains (Steel et al., 2015). Thus, each type of ecosystem differs substantially with regard to the relative influence of topography, climate and fuel on the fire regime attributes (Steel et al., 2015).

Within this framework, predictive models of burn severity may help forest managers in decision-making processes to be applied in fire-prone landscapes (Alexander et al., 2006) with two essential aims: (1) to identify priority areas for implementing pre-fire forest management strategies (Mitsopoulos et al., 2019); (2) to decide the most suitable actions based on the relative importance of the drivers contributing to high burn severity (Lecina-Diaz et al., 2014). This is particularly relevant in heterogeneous landscapes, since the location, design and implementation of fuel treatments in these areas will be widely ecosystem-specific (Lee et al., 2009; Stephens et al., 2013).

In this context, remote sensing techniques are valuable and cost-effective tools for land managers, compared to traditional field-sampling campaigns, allowing to model at large scale the relationships between the factors of the fire behavior triangle (i.e. topography, vegetation and weather) and the ecosystem impact (Viedma et al., 2015). Although field-based information provides the most direct and accurate vegetation structure measures (Zhang et al., 2013), this approach is not functional for monitoring extensive landscapes (Fernández-García et al., 2018), and usually pre-fire field data are not available at fine spatial scale (Fernández-Guisuraga et al., 2021). Recently, active remote sensors, such as airborne Light Detection and Ranging (LiDAR), have been used to establish relationships between pre-fire forest structure and burn severity with high reliability (Montealegre et al., 2014; Kane et al., 2015a; Fernandez-Manso et al., 2019; García-Llamas et al., 2019a). However, LiDAR sensors traditionally used for retrieving forest structure parameters at landscape level operate at one specific wavelength (Wallace et al., 2012), given the limited availability of commercial airborne multispectral LiDAR sensors (Morsy et al., 2017). In this sense, remote sensing data derived from passive sensors, such as spectral indices computed from multispectral satellite imagery, have been successfully used in combination with single-wavelength LiDAR data to estimate the contribution of pre-fire fuel load to burn severity (García-Llamas et al., 2019a; Viedma et al., 2020). In the context of pre-fire fuel management, several studies (e.g. Koetz et al., 2008; Chirici et al., 2013) also found that forest canopy fuel parameters were more accurately estimated by combining both LiDAR and satellite optical data. Nevertheless, broadband land surface albedo (bLSA) satellite products, accounting for the fraction of the reflected downwelling irradiance by earth surface (Tian et al., 2014) have not been yet considered in the literature as a proxy of pre-fire fuel structure to determine its influence on burn severity. Noteworthy, bLSA is more sensitive than spectral indices to subtle variations in biophysical parameters and structure of vegetation (Rodríguez-Caballero et al., 2015; Zhao et al., 2018).

Based on literature review, no study has explored up to now the potential of LiDAR and bLSA data fusion to characterize pre-fire stand structure for identifying the likelihood of high burn severity in heterogeneous landscapes as determined by variation in vegetation structure and composition. Also, studies identifying fuel drivers of burn severity as a function of ecosystem type by using specific fuel structure metrics rather than coarse-scale maps of vegetation type, are still limited (Viedma et al., 2020). Thus, the main objective of this research was to identify which particular features of vegetation structure are related to the probability of high burn severity occurrence in several fire-prone shrub and forest ecosystems within the perimeter of a large mixed-severity wildfire by means of remote sensing techniques (Sentinel-2 bLSA and LiDAR data). Topographic features were also considered in the analysis since they can assist in the selection of priority areas where vegetation structural drivers of high burn severity need to be managed to reduce the most adverse fire ecological effects.

## 2. Material and methods

The methodology comprised four steps: field measurement and mapping of burn severity, vegetation mapping at ecosystem level, computation of burn severity predictors from remote sensing data and data analysis (. 1).

### 2.1. Study area

The study was conducted in the Sierra de Cabrera mountain range (Northwest Spain; . 2), within the perimeter of a mixed severity megafire that occurred in August 2017 (between 21st and 27th) and affected 9940 ha of shrubland and tree forest ecosystems. Wildfires have been a crucial modeling process of the landscape in the study site (Fernández-Guisuraga et al., 2021), being the fire regime characterized by a high wildfire frequency (8.5 fires × 10 years$^{-1}$) (García-Llamas et al., 2020). The altitude ranges between 836 and 1938 m a.s.l. and the relief is abrupt and heterogeneous. The soils, predominantly acidic, are originated from siliceous lithologies (slates in the north and quartzite in the southernmost area) (GEODE, 2019; ITACyL, 2019). The site is located at the transition of the Mediterranean and Eurosiberian biogeographic regions (Rivas-Martínez et al., 2011). Annual mean precipitation ranges between 600 and 1500 mm and annual mean temperature between 5 and 15 °C (Ninyerola et al., 2005). The fire occurred in a year in which low precipitation rates were registered in the study site during the seasons preceding the fire date alarm (García-Llamas et al., 2020). Additionally, weather conditions during the fire progression were relatively extreme, with maximum temperatures of 35 °C, relative humidity of 35% and mean wind speed of 6 m/s, which facilitated fire spread, (García-Llamas et al., 2019b, 2020).

The mega-fire affected five different types of ecosystems dominated by either shrub or tree species (. 3): (1) gorse shrublands dominated by *Genista hystrix* Lange, (2) heath shrublands dominated by *Erica australis* L., (3) broom shrublands dominated by *Genista florida* L., (4) Pyrenean oak forests (type level 8.3 of the European Forest Types - EFTs-classification scheme; Barbati et al., 2014) dominated by *Quercus pyrenaica* Willd. and (5) Scots pine forests (EFTs level 10.4) dominated by *Pinus sylvestris* L.

### 2.2. Burn severity mapping

To evaluate burn severity, two Sentinel-2 multispectral instrument (MSI) Level 1C images covering the study area were obtained from the Copernicus Open Access Hub (2020) for both August 13th· 2017 at 11:21:21 UTC (pre-fire conditions) and September 2, 2017 at 11:21:11 UTC (post-fire conditions). These images corresponded to the available cloud cover free scenes closest to the date of the fire. Sentinel-2 MSI Level 1C scenes were topographically and atmospherically corrected

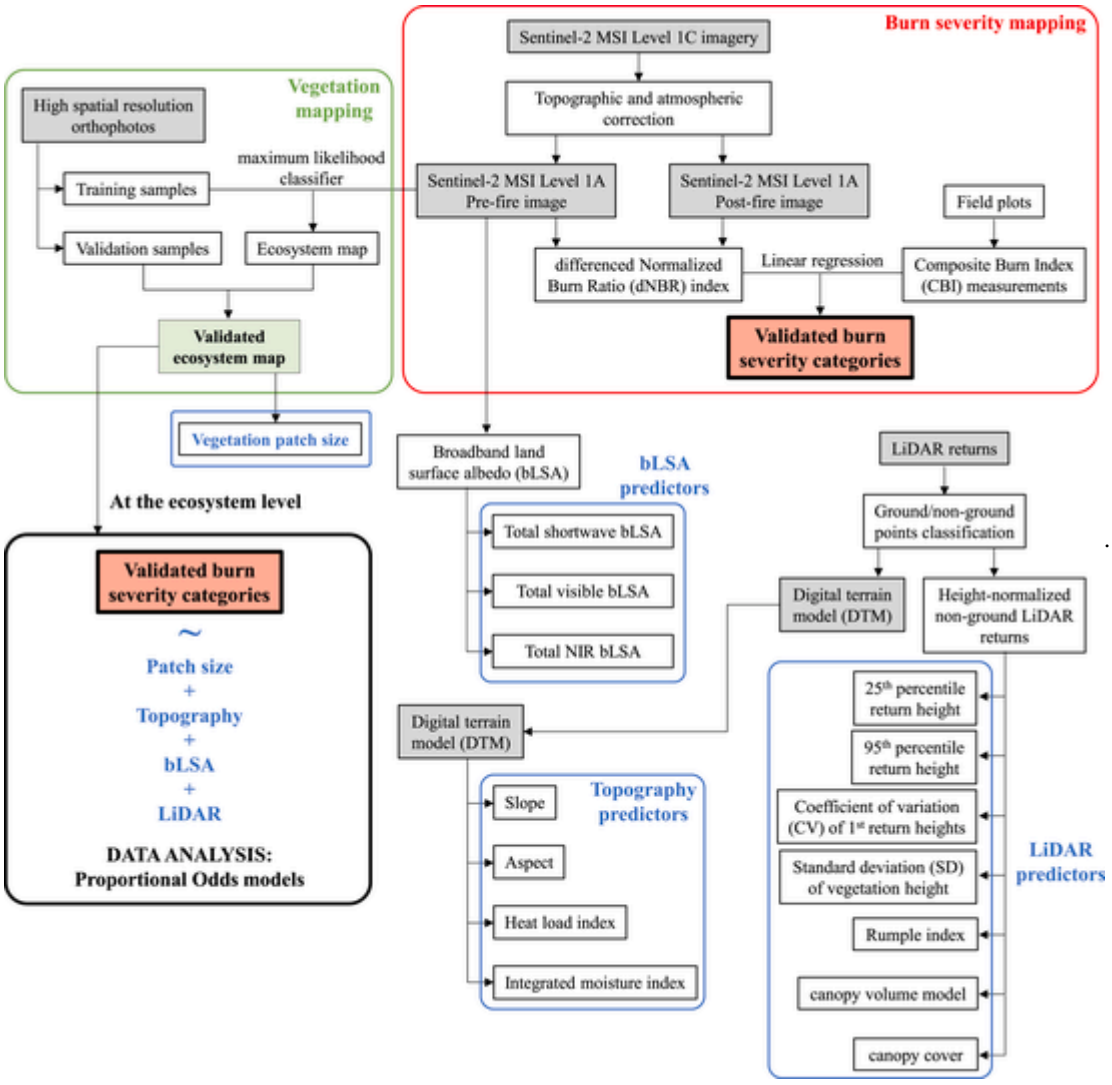


**1.** Methodology flowchart of the present study.

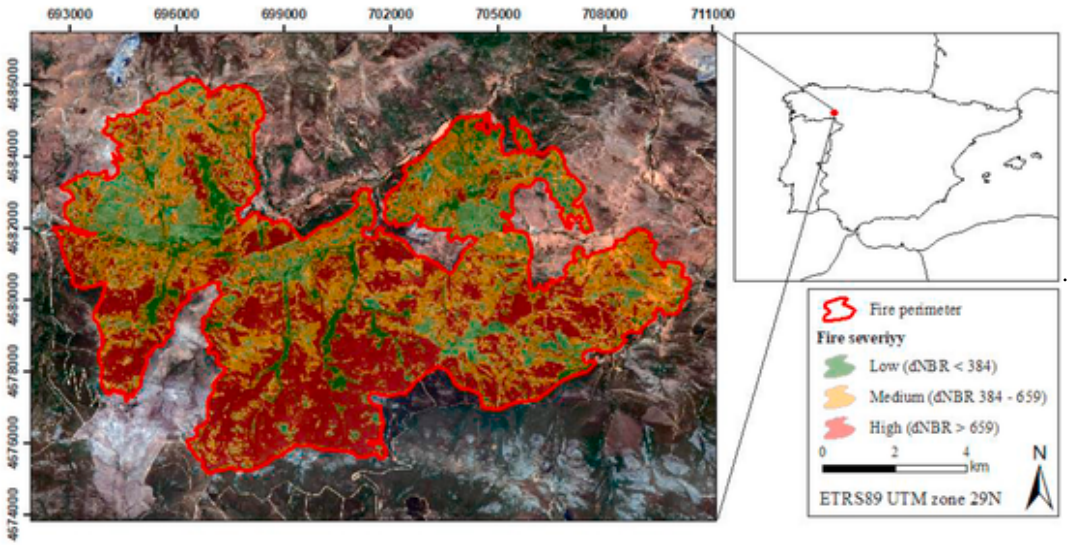


**2.** Location of the study area within the perimeter of Sierra de Cabrera wildfire (NW Spain) and spatial patterns of burn severity classified according to the difference of the Normalized Burn Ratio (dNBR) thresholds.

for surface reflectance (Level 2 A with a spatial resolution of 10 m) with the ATCOR algorithm (Richter and Schläpfer, 2018) included in PCI Geomatica 2018. Fire severity was assessed through the differenced Normalized Burn Ratio (dNBR) index scaled by $10^3$ (Key and Benson, 2006), which was computed at a spatial resolution of 10 m using the pre-fire and post-fire Sentinel-2 MSI Level 2 A scenes with bands 8 (near infrared -NIR-) and 12 (short wave infrared -SWIR-). The dNBR has been demonstrated to be the most accurate index to assess fire severity in previous research developed in the study site (García-Llamas et al., 2019c).

Additionally, two months after the wildfire, burn severity was estimated in the field using 53 plots of 30 × 30 m randomly distributed across burned homogeneous patches to ensure a uniform spectral response in the plot to be captured by Sentinel-2 pixels (Key and Benson, 2006; Fernández-García et al., 2018). A set of 19 plots were also established in unburned areas within the perimeter to be used as controls. The center of each plot was georeferenced with a Global Positioning System (GPS) receiver (Spectra Precision MobileMapper 50) with an accuracy better than 0.5 m in post-processing mode. In each field plot, initial burn severity assessment was conducted through the Composite Burn Index (CBI; Key and Benson, 2006), using the modified protocol described in Fernández-García et al. (2018) which does not include post-fire responses. Field severity was rated between 0 (unburned) and 3 (high severity). Three burn severity categories were established within the fire perimeter based on the CBI values: low (CBI < 1.25), medium (1.25 ≤ CBI ≤ 2.25) and high (CBI > 2.25). CBI thresholds correspond to those proposed by Miller and Thode (2007).

Using these CBI thresholds and a linear regression model (. 4), three dNBR burn severity categories were identified (low: dNBR < 384; medium: 384 ≤ dNBR ≤ 659; high: dNBR > 659) (. 2). The correlation between dNBR and CBI presented a coefficient of determination of 0.84.

### 2.3. Pre-fire image classification: vegetation mapping

Pre-fire Sentinel-2 MSI Level 2 A image at a spatial resolution of 10 m was classified by means of a maximum likelihood (ML) classifier (Strahler, 1980) approach to perform vegetation mapping. ML is a parametric classifier in which the spectral data within each class is assumed to be normally distributed (Wang et al., 2004). The probability of a pixel to belong to a specific class is computed through the mean vectors of the classes and the covariance matrix, as well as the class frequency to estimate the prior probability of each class (Radoux et al., 2014). ML is one of the most used algorithms in remote sensing data classification as it usually provides accurate results when using a large number of training samples (Radoux et al., 2014; Burai et al., 2015), and avoids data overfitting (Yang et al., 2020). Moreover, this classifier is an appropriate algorithm to use with not too fine-grained imagery (spatial resolution lower than 1 m) in which the class distributions are not highly spread and the noise is generally low (Volpi et al., 2013). Six classes were considered to classify the satellite imagery based on field knowledge: gorse, heath, broom, oak and pine ecosystems, as well as rock outcrops. Training samples were delineated as polygons through the pre-fire image within homogeneous patches fairly distributed across the fire perimeter. For each class, training samples contained at least one thousand pure pixels. Pre-fire orthophotographs (year 2017) at very high spatial resolution (0.5 m) of the Spanish Aerial Orthophotography National Planning (PNOA, 2020) supplied by the Spanish National Center of Geographic Information (CNIG, 2020) were used to assist training samples delineation together with field knowledge. A spatial majority filter was applied to the classified image with a kernel size of 3 × 3 pixels to reduce classification noise. To assess the accuracy of the final map, overall classification accuracy and Kappa statistic of the confusion matrix were quantified using a validation dataset of one thousand pixels randomly sampled across the same orthophotographs. Finally, the area of every patch (ha) was computed from the output of the classification algorithm for each ecosystem.

### 2.4. Burn severity predictors

#### 2.4.1. Topographic data

A digital terrain model (DTM) with a spatial resolution of 10 m, computed from LiDAR data (see section 2.4.3), was used to derive a set of topographic variables that have a well-known impact on burn severity (Broncano and Retana, 2004; Flatley et al., 2011; Fang et al., 2018) (Table 1): (1) slope, in degrees; (2) aspect, transformed to a continuous variable ranging between 0 (NNE slopes) and 1 (SSW slopes) (Roberts and Cooper, 1989); (3) heat load index (McCune and Keon, 2002), based on geographic latitude, aspect and steepness of the slope, with the highest values corresponding to the warmest southwest facing slopes; and, (4) integrated moisture index (Iverson et al., 1997), which estimates potential soil moisture based on solar radiation, flow accumulation and landscape curvature.

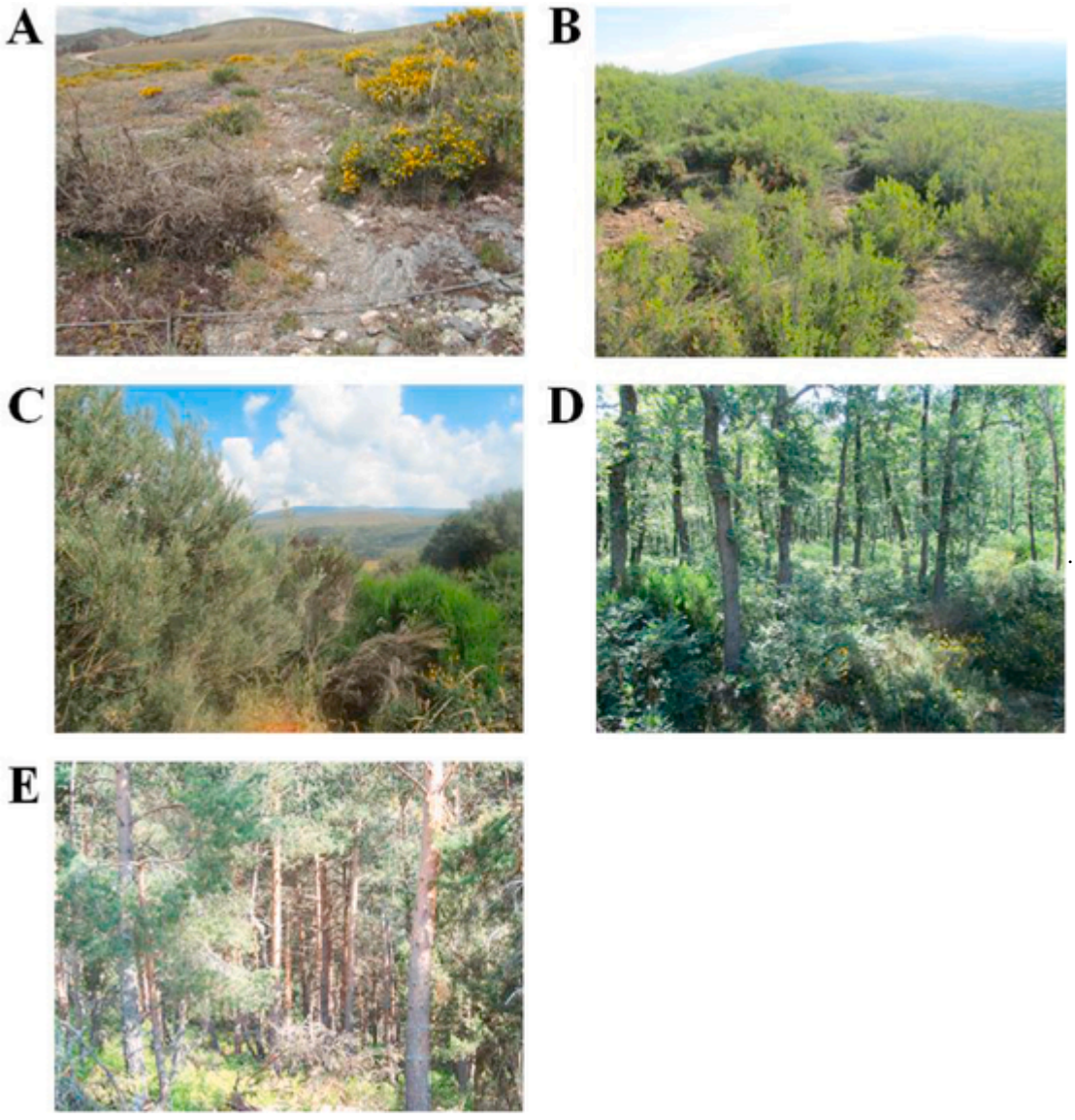


**3.** Photographs of the five ecosystems affected by the mega-fire: (A) gorse shrublands dominated by *Genista hystrix*; (B) heath shrublands dominated by *Erica australis;* (C) broom shrublands dominated by *Genista florida;* (D) Pyrenean oak forest dominated by *Quercus pyrenaica*; and (E) Scots pine forest dominated by *Pinus sylvestris* L.

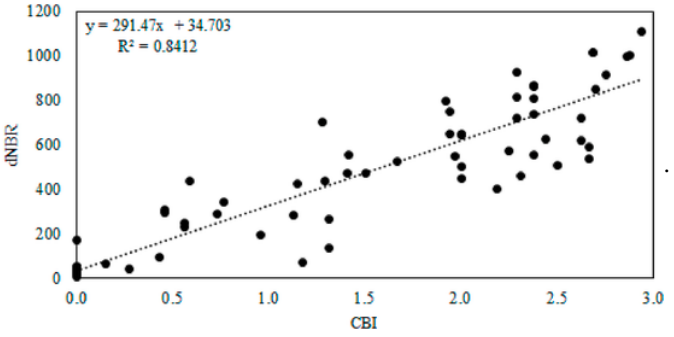


**4.** Linear model used to compute dNBR thresholds from CBI burn severity categories.

*2.4.2. bLSA as a measure of vegetation structure and composition*

The surface reflectance bands of the pre-fire Sentinel-2 MSI Level 2 A image were used to retrieve several bLSA metrics (Table 1) following the approaches proposed by Liang (2001), Li et al. (2018) and Vanino et al. (2018).

(1) Liang (2001) provided several albedo conversion equations for Landsat Thematic Mapper (TM)/Enhanced Thematic Mapper Plus (ETM +) sensors based on radiative transfer simulations using a wide range of reflectance spectra (Liang et al., 2012). The equation coefficients specified by Liang (2001) for Landsat TM/ETM + and the best matching Sentinel-2 surface reflectance bands (Naegeli et al., 2017) were used to retrieve total shortwave bLSA metric, three visible bLSA metrics (total, direct and diffuse) and three NIR bLSA metrics (total, direct and diffuse). Hereafter referred to as Liang bLSA metrics.

(2) Li et al. (2018) generated specific conversion equations for Sentinel-2 surface reflectance bands through radiative transfer simulations. These equations were used in this study to retrieve total shortwave bLSA, total visible bLSA and total NIR bLSA. Hereafter referred to as Li bLSA metrics.

(3) Total shortwave bLSA was also retrieved following the methodology by Vanino et al. (2018) who used weighting coefficients that represent the fraction of solar radiation within the spectral width of each Sentinel-2 surface reflectance band. Hereafter referred to as Vanino bLSA metric.

**Table 1**
Groups of burn severity predictors considered in this study.

| Topographic variables | |
|---|---|
| **slope (º)** | |
| transformed aspect | Roberts and Cooper (1989) |
| heat load index | McCune and Keon (2002) |
| integrated moisture index | Iverson et al. (1997) |
| **broadband Land Surface Albedo (bLSA) metrics** | |
| Liang total shortwave bLSA | Liang (2001) |
| Liang total visible bLSA | Liang (2001) |
| Liang direct visible bLSA | Liang (2001) |
| Liang diffuse visible bLSA | Liang (2001) |
| Liang total NIR bLSA | Liang (2001) |
| Liang direct NIR bLSA | Liang (2001) |
| Liang diffuse NIR bLSA | Liang (2001) |
| Li total shortwave bLSA | Li et al. (2018) |
| Li total visible bLSA | Li et al. (2018) |
| Li total NIR bLSA | Li et al. (2018) |
| Vanino total shortwave bLSA | Vanino et al. (2018) |
| **LiDAR metrics** | |
| 25th percentile return height | |
| 95th percentile return height | |
| coefficient of variation (CV) of first return heights | |
| standard deviation (SD) of vegetation height | |
| rumple index | Kane et al. (2010) |
| canopy volume model | McGaughey (2018) |
| canopy cover | Kane et al. (2008) |

See Liang (2001), Li et al. (2018) and Vanino et al. (2018) for the detailed bLSA retrieval equations.

#### 2.4.3. LiDAR data as a measure of vegetation structure

LiDAR data were acquired for the period between October 2010 and November 2010 from PNOA (2020). Data were collected using a Leica ALS50 sensor aboard a fixed-wing aircraft, with a side overlap of 25% and a maximum scan angle of ±25°from nadir. The LiDAR sensor operated with a pulse frequency of 90.85 kHz on average, producing a mean first-return point density of 0.54 $m^{-2}$ (nominal pulse spacing of 1.36 m). The sensor captured a maximum of four returns per pulse.

Areas affected by fire events occurred between 2010 (LIDAR data collection) and 2017 (fire event) were discarded from further analyses to avoid large changes in vegetation structural attributes, following the same criteria than other authors (Kane et al., 2013; Fernandez-Manso et al., 2019; García-Llamas et al., 2020). Both the nature of fuels and its spatial distribution were confirmed to be similar in unburned areas during the 7-year time lag through photointerpretation of PNOA orthophotographs dated between 2008 and 2015 (García-Llamas et al., 2020). Thus, LiDAR data collected in 2010 were assumed to be representative of pre-fire vegetation conditions in August 2017 according to Fernandez-Manso et al. (2019).

The LiDAR return point cloud was processed using the US Forest Service's FUSION software package Version 3.80 (McGaughey, 2018). A DTM at 10 m of spatial resolution was computed from the filtered ground returns of the LiDAR point cloud (García-Llamas et al., 2019a). LiDAR returns were then normalized to heights above ground by subtracting, from each first return, the underlying DTM elevation (Kane et al., 2013; García-Llamas et al., 2019a). A set of LiDAR metrics closely related with vegetation structure were computed from the returns above ground and aggregated within a 10 m grid to match Sentinel-2 MSI Level 2 A spatial resolution (Table 1): (1) 25th percentile return height, which has proved to be an adequate metric to estimate canopy base height (Andersen et al., 2005; Kelly et al., 2018); (2) 95th percentile return height, as a measure of canopy mean height (Kane et al., 2013; Kwak et al., 2014); (3) coefficient of variation (CV) of first return heights, which is a sensitive metric to canopy vertical complexity (Kane et al., 2010); (4) standard deviation (SD) of vegetation height within a 3 × 3 pixel moving window, as a measure of canopy roughness; (5) rumple index (surface area ratio), which measures the horizontal and vertical variation of vegetation structure (Kane et al., 2010) and was computed as the ratio of a 3D canopy surface model (CSM) at 1 m of spatial resolution (Kane et al., 2013) to the area of the underlying DTM; (6) canopy volume model, computed from the vertices of a triangular irregular network of top of canopy three dimensional points to the area of the DTM grid size, and related to canopy density (Kane et al., 2008; McGaughey, 2018); and, (7) canopy cover, as the proportion of first returns higher than 20 cm above ground surface (Kane et al., 2008, 2010). The canopy cover metric was related to understory and canopy vegetation cover, rather than just to canopy cover, since height-break was set to 20 cm (García-Llamas et al., 2020).

### 2.5. Statistical analysis

The categorized burn severity was selected as response variable since the primary objective of this study was to determine the influence of topography and pre-fire vegetation structure on the probability of a pixel to be burned at a high severity. Although the burn severity actually occurs on a continuum scale, its categorization improves the communication of operational data required by resource managers (Rogan and Franklin, 2001). In fact, the prediction of high burn severity outcome is a key target in pre-fire decision making (Miller and Thode, 2007). The ordinal nature of the response variable (low: dNBR < 384; medium: 384 ≤ dNBR ≤ 659; high: dNBR > 659) required the choice of ordinal regression as the modeling technique to be applied in this study (Guisan and Harrell, 2000). Specifically, a proportional odds (PO) model was used given that the model is theoretically invariant to reversals of the response categories (Walker and Duncan, 1967).

To avoid further problems of multicollinearity among the predictors, bivariate Pearson correlations were previously evaluated to identify strongly correlated groups of burn severity predictors ($r_{Pearson} > 0.7$). Within each group of correlated predictors, the predictor with the highest predictive discrimination ability evaluated through Nagelkerke R-Square ($R^2$) (Nagelkerke, 1991) in univariate PO models was preserved for subsequent analysis.

For each ecosystem, univariate and multivariate PO models were fitted separately for each family of burn severity drivers (topographic, pre-fire bLSA and pre-fire LiDAR metrics) and altogether, in a global multivariate model including all uncorrelated predictors from all categories of burn severity drivers. A model calibration dataset was built for each ecosystem consisting of three hundred random points, separated at least 100 m and equally distributed within each burn severity category, discarding burned areas during the 7-year time mismatch between LiDAR data acquisition and fire date. The relative importance of the predictors in the global multivariate model was assessed through Wald $\chi^2$ statistic (Mon et al., 2012). Multivariate and global multivariate PO models were calibrated retaining only significant predictors (p Wald $\chi^2 < 0.05$) using a forward selection procedure (Eskelson et al., 2012). Model validation was conducted through 10-fold cross-validation repeated 10 times and averaging the unbiased validation statistics over the repetitions (Huy et al., 2019). Overfitting corrected $R^2$ was provided as a measure of quality of ordinal predictions (Guisan and Harrell, 2000). Also, the models were tested on independent data with the same size and sampling strategy as the calibration dataset. A minimum distance of 100 m between calibration and validation points was ensured. The PO models were applied to the independent dataset, generating dNBR category predictions based on the output probability for each observation (the dNBR category with the largest predicted probability value is assigned as the predicted category; Christensen, 2018). The overall classification accuracy was computed from the predicted versus observed dNBR category of the confusion matrix. Statistical analyses were conducted in R (R Core Team, 2019) using "MASS"

(Venables and Ripley, 2002), "rms" (Harrell, 2019), "ordinal" (Christensen, 2019) and "effects" (Fox and Hong, 2009; Fox and Weisberg, 2019) packages.

## 3. Results

The five ecosystems occurring in the study area were successfully classified at 10 m of spatial resolution (overall accuracy = 0.91; Kappa index = 0.89). None of the classes was significantly under or overestimated (. 5A and B).

Over than 37% of the surface of the study site (3526 out of 9940 ha) was burned at high severity, being the ecosystems dominated by heath, Scots pine and Pyrenean oak species the most affected by high burn severity (81%, 80% and 53% of the ecosystem surface, respectively). Broom ecosystem was predominantly burned at medium burn severity (surface of 50%), while gorse ecosystem was burned mainly at low severity (surface of 63%) (Table 2).

Based on classification accuracy and overfitting corrected $R^2$ of multivariate models for each group of burn severity predictors (Table 3), vegetation structure properties derived from LiDAR data were the most important drivers of burn severity in Pyrenean oak and Scots pine forest ecosystems (accuracy and $R^2$ higher than 68% and 0.52, respectively). By contrast, the contribution of LiDAR metrics for explaining burn severity in shrub ecosystems was limited. bLSA was the strongest predictor of burn severity in gorse (accuracy = 77% and $R^2$ = 0.70) and broom (accuracy = 68% and $R^2$ = 0.58) shrub ecosystems. Vegetation patch size was also a relevant controlling factor of burn severity in such ecosystems (accuracy higher than 61% and $R^2$ = 0.43). Topography characteristics featured accuracies higher than 60% in forest ecosystems and 40–50% in shrub ecosystems.

The global burn severity model (i.e. including all categories of burn severity drivers) for each ecosystem registered overall classification accuracies ranging from 71% to 82% (Table 4). In gorse shrub ecosystems, areas with low shortwave and visible bLSA registered high probabilities of being burned at high severity (. 6A). Vegetation patch size played a minor role in the global model (Table 5) due to the overwhelming effect of bLSA metrics. Similar patterns were observed in broom shrub ecosystems, but, in addition, a high canopy volume was strongly related to stands severely affected by fire (Table 5 and . 6C). Heath shrub ecosystems characterized by low rumple values were highly prone to high

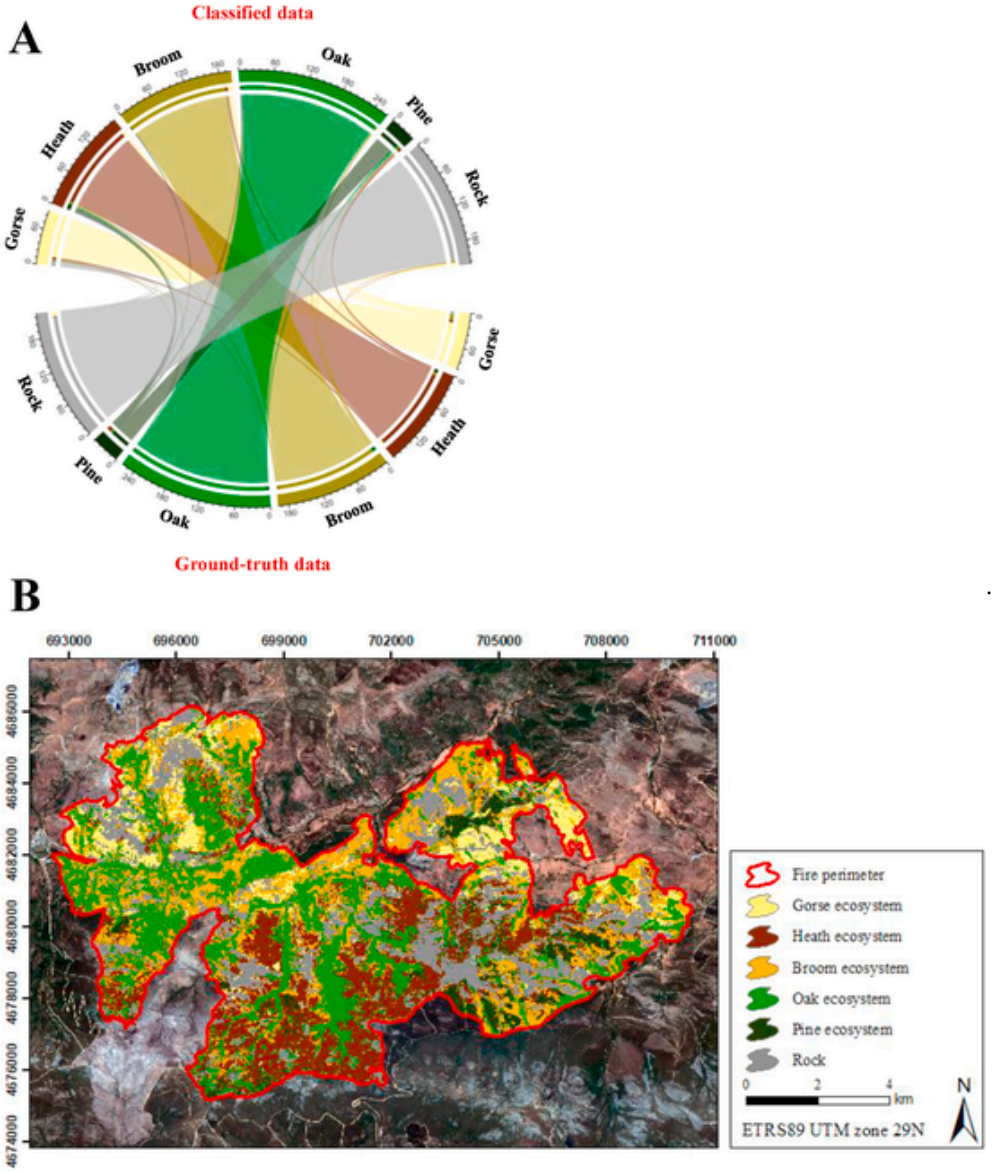


**5.** Visualization of the confusion matrix by means of a chord diagram (A) and pre-fire ecosystem classification map computed from the pre-fire Sentinel-2 MSI Level 2 A scene at 10 m of spatial resolution using a maximum likelihood (ML) algorithm (B).

**Table 2**
Area (in hectares) affected by each burn severity category defined by difference of the Normalized Burn Ratio (dNBR) thresholds.

| BURN SEVERITY | ECOSYSTEM AFFECTED AREA (ha) | | | | | |
|---|---|---|---|---|---|---|
| | Gorse | Heath | Broom | Oak | Pine | Total |
| Low (dNBR < 384) | 562.32 (63%) | 53.19 (3%) | 314.37 (16%) | 308.43 (23%) | 30.24 (6%) | 2621.79 (27%) |
| Medium (dNBR 384–659) | 309.96 (35%) | 292.86 (16%) | 993.87 (50%) | 314.64 (24%) | 63.45 (14%) | 3409.65 (36%) |
| High (dNBR > 659) | 16.56 (2%) | 1433.25 (81%) | 681.39 (34%) | 715.50 (53%) | 371.88 (80%) | 3526.11 (37%) |
| Total burned area | 888.84 | 1779.30 | 1989.63 | 1338.59 | 465.57 | |

burn severity, particularly those located in steep and southwest facing slopes (Table 5 and . 6B). Severe fire effects in Pyrenean oak ecosystems were also closely associated with high canopy volumes (. 6D), showing this variable by far the most important contribution in the global model (Table 5). In Scots pine ecosystems, 25th percentile return height LiDAR metric was the most relevant property of the stand structure for explaining burn severity (Table 5), this metric being inversely related with the probability of high burn severity outcome (. 6E).

## 4. Discussion

The results of this study give light to the relevance of pre-fire fuel structure parameters and topography as drivers of high burn severity across different types of ecosystems. This understanding is crucial for decision-making strategies regarding where and how to implement pre-fire management actions aimed to reduce the most adverse ecological effects of severe wildfires (Estes et al., 2017), which are ecosystem-dependent (Stephens et al., 2013).

**Table 3**
Univariate, multivariate and global burn severity model performance (overfitting corrected $R^2$ and overall classification accuracy -Acc-) for each occurring ecosystem within the perimeter of the Sierra de la Cabrera wildfire. Topography and vegetation structure categories comprise only uncorrelated burn severity predictors.

| | | GORSE | | HEATH | | BROOM | | OAK | | PINE | |
|---|---|---|---|---|---|---|---|---|---|---|---|
| | | $R^2$ | Acc | $R^2$ | Acc | $R^2$ | Acc | $R^2$ | Acc | $R^2$ | Acc |
| **Topography** | Slope | 0.21 | 0.42 | 0.09 | 0.44 | 0.15 | 0.34 | 0.18 | 0.41 | 0.29 | 0.56 |
| | transformed aspect | 0.05 | 0.29 | 0.06 | 0.27 | 0.03 | 0.34 | 0.11 | 0.37 | 0.12 | 0.31 |
| | heat load index | 0.18 | 0.46 | 0.15 | 0.34 | 0.08 | 0.32 | 0.24 | 0.49 | 0.30 | 0.54 |
| | integrated moisture index | 0.05 | 0.22 | 0.15 | 0.18 | 0.07 | 0.23 | 0.08 | 0.16 | 0.07 | 0.18 |
| | **topographic multivariate model** | **0.33** | **0.48** | **0.24** | **0.51** | **0.29** | **0.43** | **0.39** | **0.61** | **0.40** | **0.66** |
| **Vegetation structure** | **patch size** | **0.43** | **0.67** | **0.18** | **0.50** | **0.43** | **0.61** | **0.06** | **0.34** | **0.11** | **0.45** |
| | Liang total shortwave bLSA (canopy cover) | 0.39 | 0.57 | 0.23 | 0.43 | 0.20 | 0.53 | 0.14 | 0.38 | 0.29 | 0.39 |
| | Liang total visible bLSA (canopy cover) | 0.61 | 0.67 | 0.20 | 0.41 | 0.52 | 0.56 | 0.07 | 0.39 | 0.36 | 0.42 |
| | **albedo multivariate model** | **0.70** | **0.77** | **0.19** | **0.43** | **0.58** | **0.68** | **0.18** | **0.40** | **0.35** | **0.49** |
| | rumple index (3D vegetation heterogeneity) | 0.07 | 0.30 | 0.25 | 0.43 | 0.10 | 0.42 | 0.35 | 0.63 | 0.35 | 0.51 |
| | canopy volume | 0.28 | 0.49 | 0.27 | 0.47 | 0.35 | 0.51 | 0.25 | 0.54 | 0.11 | 0.43 |
| | SD of vegetation height (canopy roughness) | 0.11 | 0.39 | 0.24 | 0.42 | 0.07 | 0.41 | 0.14 | 0.49 | 0.18 | 0.37 |
| | CV of return heights (canopy vertical complexity) | 0.13 | 0.38 | 0.04 | 0.37 | 0.03 | 0.30 | 0.20 | 0.50 | 0.28 | 0.43 |
| | 25th percentile return height (canopy base height) | 0.04 | 0.27 | 0.16 | 0.38 | 0.07 | 0.40 | 0.16 | 0.38 | 0.48 | 0.63 |
| | 95th percentile return height (canopy mean height | 0.12 | 0.39 | 0.28 | 0.41 | 0.08 | 0.37 | 0.20 | 0.50 | 0.31 | 0.54 |
| | **LiDAR multivariate model** | **0.28** | **0.49** | **0.33** | **0.52** | **0.32** | **0.51** | **0.52** | **0.68** | **0.59** | **0.71** |
| | **GLOBAL MODEL** | **0.70** | **0.80** | **0.63** | **0.71** | **0.67** | **0.77** | **0.66** | **0.79** | **0.80** | **0.82** |

**Table 4**
Global burn severity model for each ecosystem present within the perimeter of the Sierra de la Cabrera wildfire.

| ECOSYSTEM | | GORSE | | HEATH | | BROOM | | OAK | | PINE | |
|---|---|---|---|---|---|---|---|---|---|---|---|
| ACCURACY | | 0.80 | | 0.71 | | 0.79 | | 0.79 | | 0.82 | |
| COEFFICIENTS | | value | p-value | value | p-value | value | p-value | value | p-value | value | p-value |
| **Topography** | Slope | 0.0951 | <0.01 | 0.1852 | <0.001 | 0.0696 | <0.05 | 0.1041 | <0.001 | – | – |
| | transformed aspect | 1.1271 | <0.05 | – | – | – | – | 3.3960 | <0.001 | 6.5457 | <0.001 |
| | heat load index | 11.5564 | <0.001 | 12.2503 | <0.001 | – | – | 24.0315 | <0.001 | 44.1286 | <0.001 |
| | integrated moisture index | – | – | – | – | – | – | – | – | – | – |
| **Vegetation structure** | patch size | −0.0581 | <0.01 | 0.0188 | <0.001 | 0.0477 | <0.01 | – | – | 0.0562 | <0.001 |
| | Liang total shortwave bLSA (canopy cover) | −181.07 | <0.001 | – | – | −66.123 | <0.001 | – | – | – | – |
| | Liang total visible bLSA (canopy cover) | −318.80 | <0.001 | −75.37 | <0.001 | −222.46 | <0.001 | – | – | – | – |
| | rumple index (3D vegetation heterogeneity) | – | – | −6.5802 | <0.001 | – | – | −0.2703 | <0.05 | −0.8033 | <0.01 |
| | canopy volume | 0.0151 | <0.001 | 0.0131 | <0.001 | 0.0290 | <0.001 | 0.0241 | <0.001 | – | – |
| | SD of vegetation height (canopy roughness) | – | – | – | – | – | – | – | – | – | – |
| | CV of return heights (canopy vertical complexity) | – | – | – | – | – | – | – | – | – | – |
| | 25th percentile return height (canopy base height) | – | – | – | – | – | – | – | – | −0.7923 | <0.05 |
| | 95th percentile return height (canopy mean height) | – | – | – | – | – | – | – | – | – | – |
| INTERCEPTS | | | | | | | | | | | |
| | low\|medium | 9.4500 | <0.001 | 6.3124 | <0.001 | 5.6512 | <0.001 | 20.6142 | <0.001 | 18.2139 | <0.001 |
| | medium\|high | 13.1308 | <0.001 | 9.1374 | <0.001 | 8.9659 | <0.001 | 23.2188 | <0.001 | 22.4609 | <0.001 |

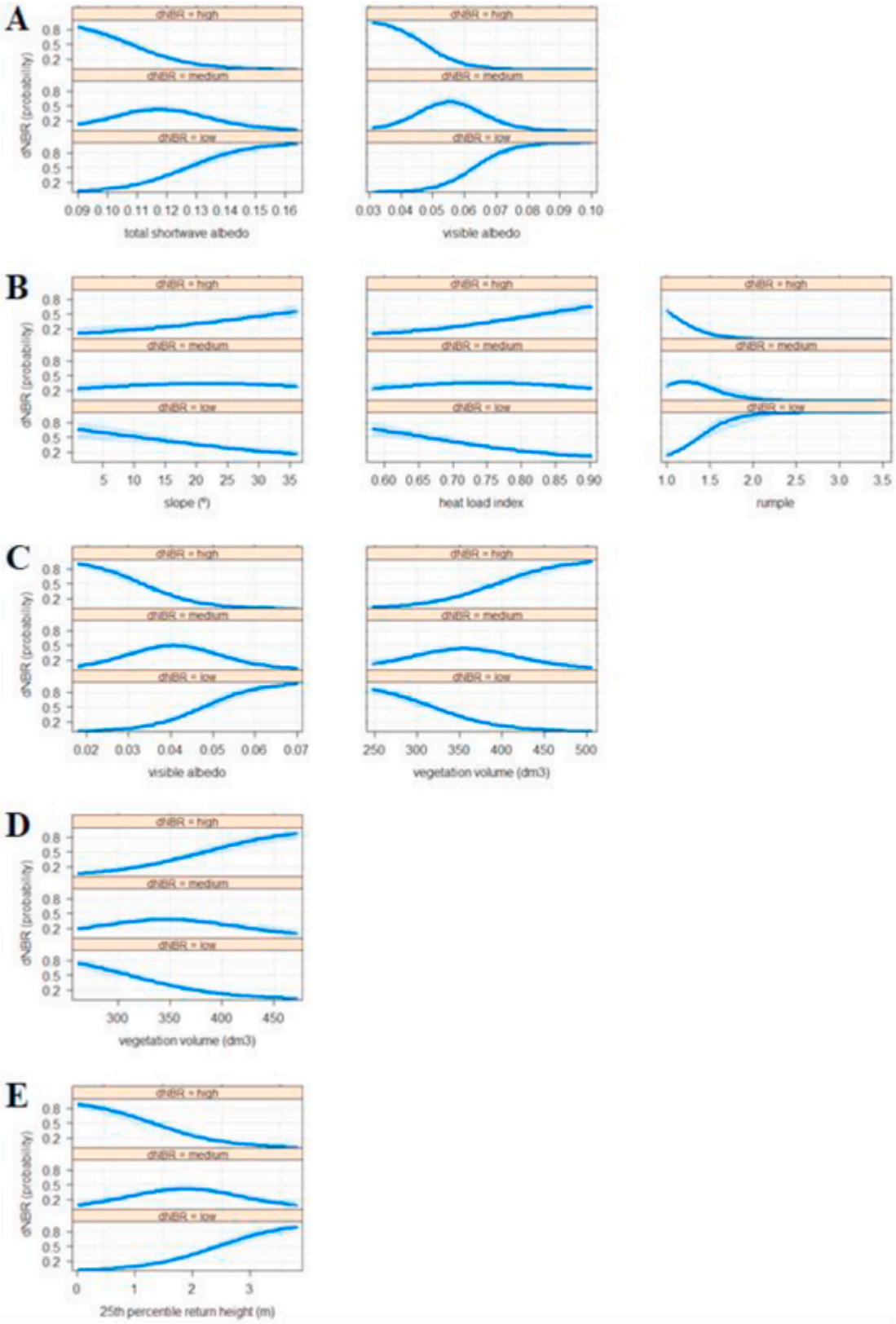


**Fig. 6.** Predicted probabilities of classification into high, medium and low burn severity classes for burn severity predictors with the highest relative importance in the global model for gorse (A), heath (B), broom (C), oak (D) and pine (E) ecosystems. Relative importance threshold for each ecosystem was established on the basis on predictors with 20% more importance than the next most contributing variable (Table 5), or if this condition was not met, all predictors with more than 20% relative importance were shown.

**Table 5**
Importance of the predictors on the global model measured by the Wald $\chi^2$ statistic.

| | | GORSE | HEATH | BROOM | OAK | PINE |
|---|---|---|---|---|---|---|
| Topography | Slope | 1.72 | 36.57 | 7.78 | 18.27 | – |
| | transformed aspect | 1.35 | – | – | 9.26 | 28.99 |
| | heat load index | 2.97 | 24.58 | – | 20.06 | 35.29 |
| | integrated moisture index | – | – | – | – | – |
| Vegetation structure | patch size | 6.06 | 9.32 | 2.67 | – | 12.91 |
| | Liang total shortwave bLSA (canopy cover) | 30.60 | – | 5.10 | – | – |
| | Liang total visible bLSA (canopy cover) | 55.24 | 17.86 | 50.57 | – | – |
| | rumple index (3D vegetation heterogeneity) | – | 20.90 | – | 19.81 | 7.40 |
| | canopy volume | 12.50 | 17.79 | 46.82 | 42.00 | – |
| | SD of vegetation height (canopy roughness) | – | – | – | – | – |
| | CV of return heights (canopy vertical complexity) | – | – | – | – | – |
| | 25th percentile return height (canopy base height) | – | – | – | – | 55.80 |
| | 95th percentile return height (canopy mean height) | – | – | – | – | – |

### 4.1. Multi-ecosystem evaluation of high burn severity drivers

Large extensions of ecosystems dominated by *Pinus sylvestris*, *Erica australis* and *Quercus pyrenaica* were burned at high severity. In fact, pine forests are highly prone to the occurrence of stand-replacing crown fires, as evidenced by others authors (e.g. Broncano and Retana, 2004; García-Llamas et al., 2019a), Scots pine forests dominated by *Pinus sylvestris* being one of the most susceptible European pine ecosystems to crown damage (Crecente-Campo et al., 2009). The high susceptibility of *Erica australis* heathlands to severe fires can be explained by: (1) a high surface area to volume ratio of live fuel (Paula and Ojeda, 2006); (2) a high amount of dead fuel (Vega, 2007); and (3) the even-aged characteristics and homogeneous structure of *Erica australis* stands (Keeley, 2002). Similarly to other studies (e.g. Fernandes et al., 2010; Fernandes, 2013), the surface affected by high burn severity in oak ecosystems was substantially lower than in pine ecosystems. This finding could be associated with the higher amount of live and dead fuel moisture content, the lesser flammable litter (Fernandes et al., 2010) and the higher site humidity (Quintano et al., 2019) as compared to conifer forests. Despite this, the prevailing young oak stands that hold high fuel load at a low height as a consequence of the high fire frequency of the landscape (González and Pukkala, 2007; Catry et al., 2010), were still prone to high burn severity. Under relatively extreme fire weather conditions, similar burn severity patterns could be expected in related Mediterranean ecosystems as emphasized by Oliveras et al. (2009) and Fernandes et al. (2016).

Previous research in this area (García-Llamas et al., 2020) demonstrated the significant effect of pre-fire vegetation structure parameters and topography on burn severity. In the present paper, the importance of those drivers was found to be strongly ecosystem-specific. Burn severity in Pyrenean oak and Scots pine forests was mainly driven by fuel arrangement parameters that were computed from LiDAR returns. Several studies have used LiDAR data to assess fire effects on forest vegetation (e.g. Wulder et al., 2009; Kane et al., 2013; Fernandez-Manso et al., 2019). However, little research (García-Llamas et al., 2019a, 2020) have found significant relationships, as those attained in this study, between low pulse density LiDAR metrics and burn severity in fire-prone ecosystems. In addition, this is the first research that has demonstrated the potential of a three-dimensional canopy volume model computed from LiDAR data for pre-fire management decision-making. In young Pyrenean oak stands, closed canopies with high aerial fuel continuity promoted an extreme fire behavior as evidenced by the high contribution of the canopy volume metric in the modeling approach, which largely overwhelmed the contribution of other canopy metrics. In this sense, Perchemlides et al. (2008) also evidenced that oak stands in western United States with high live and dead canopy fuel densities were more prone to stand-replacing crown fires. By contrast, differences in the fuel arrangement between Scots pine and Pyrenean oak stands, such as lower stand density in the study site and a more stratified canopy architecture of the former, enabled high burn severity to be better predicted by the vertical distribution of the fuel load (Mitsopoulos and Dimitrakopoulos, 2007; Fernández-Alonso et al., 2017). Indeed, low 25th percentile return heights in Scots pine ecosystems, directly related to crown base height (Kelly et al., 2018), enhanced vertical connectivity with understory fuels, and were strongly associated with an increased probability of high burn severity. Although *Pinus sylvestris* features an efficient self-pruning mechanism of dead branches below the living crown (Mäkinen and Colin, 1999), the branches could remain attached to the stem base for a long period of time, especially in old and dense stands (Mäkinen and Song, 2002), serving as ladder fuel with high susceptibility to crowning. García-Llamas et al. (2020) also identified a significant relationship between 25th percentile metric and burn severity (relative importance of 24% compared to 56% in this study, using different modeling approaches) in a pine ecosystem dominated by *Pinus halepensis* Mill. Conversely, a lack of burn severity predictability of this metric was observed in conifer stands of Sierra Nevada, United States (Kane et al., 2015b). The authors attributed it to the large scale of variability of burn severity patterns in the site as compared to the size of the used LiDAR grid (30 m). Nevertheless, the much finer scale (10 m) used in the present study was suitable for the assessment of burn severity drivers at ecosystem level. For the case of heathland ecosystems dominated by *Erica australis*, horizontal and vertical fuel continuity, measured by rumple LiDAR index, increased the likelihood of high burn severity as demonstrated in previous field-based studies (Bradstock et al., 2002; Plucinski, 2003). Indeed, homogeneous mature heath stands tend to accumulate fine dead fuel in the lowest stratum as a consequence of lower light availability (Quintano et al., 2019), which is associated with an increased likelihood of high burn severity (Baeza et al., 2006).

On their hand, bLSA products gained special relevance as a measure of pre-fire vegetation structure controlling high burn severity in gorse and broom shrublands, which are characterized by a sparsely vegetation cover. Although bLSA metrics have not been used before in burn severity assessment, several studies have evaluated the relationship between ecosystem structure and albedo. In this sense, strong relationships between vegetation cover and bLSA are expected in patchy vegetated areas due to the larger spectral changes associated to variations in vegetation cover as compared to more densely vegetated areas (Tian et al., 2014). Also, increased aboveground biomass and vegetation cover values are often related with declines in both total shortwave and visible bLSA (Lukeš et al., 2013; Kuusinen et al., 2016), what is characterizing gorse and broom areas prone to high burn severity.

In accordance with the results obtained by García-Llamas et al. (2019a), topographic effects were outperformed by vegetation structure metrics, except in heath ecosystems dominated by *Erica australis*. In this case, steep and southwest facing slopes could be directly related to high burn severity occurrence, since this terrain configuration promotes both the presence of drier fuels (Alexander et al., 2006; Dillon et al., 2011) and the preheating of fuels located uphill (Maingi and Henry, 2007). However, these results should be interpreted with caution, since

burning conditions related to weather properties and fire propagation variables may exert dominant control over burn severity in relation to topography (Viedma et al., 2015; García-Llamas et al., 2020), particularly under extreme climatic conditions (Turner and Romme, 1994).

Despite the promising findings reported in this research regarding novel LiDAR and bLSA metrics in the field of fire behavior prediction, some limitations should be highlighted: (1) the use of LiDAR data with a higher pulse density could have improved the accuracy of metrics in ecosystems dominated by low height vegetation (Jakubowski et al., 2013); (2) only properties that could be controlled through management strategies were evaluated, such as pre-fire vegetation structure or topography to prioritize actions (Parks et al., 2018), despite fire weather variables are key drivers of fire severity and may shift the effect of other drivers (Dillon et al., 2011; Viedma et al., 2015; Estes et al., 2017). Several studies have successfully related weather and fire propagation variables with burn severity (e.g. Viedma et al., 2015; 2020; García-Llamas et al., 2019a) using a single automated weather station or coarse satellite data. However, many weather predictors operate at macro-scale (Costa et al., 2011) and, therefore, they do not match the ecosystem spatial scale of the study site. Besides, high spatial resolution weather data are not usually available at the high spatial resolution required for studies at ecosystem level (Fang et al., 2018). Downscaling coarse weather data, such as that provided by MODIS or Meteosat, would not provide enough variability at the scale of the analysis to represent the actual meteorological conditions within each ecosystem (Fang et al., 2018; Mitsopoulos et al., 2019). By contrast, even coarse weather data becomes mandatory in the burn severity assessment at synoptic spatial scales because of the increased fire weather variability across large ecoregions (Park et al., 2018).

### 4.2. Fuel management implications

The proposed LiDAR and bLSA data fusion approach could assist forest managers to implement fire-smart forest strategies aimed at reducing the risk of severe fire events and enhancing ecosystem resilience (Corona et al., 2015). The results of this study provided evidence on the need of reducing the fuel load and modifying the fuel arrangement, particularly in the most prone ecosystems to high burn severity. In Scots pine ecosystems, the use of 25th percentile return height LiDAR metric would be advisable to identify stands where it is necessary to break up fuel vertical continuity, and reduce the risk of active crown fire initiation (Agee et al., 2000). Hence, one of the most effective measures to minimize the probability of severe fires in these ecosystems is associated with the increase of the canopy base height by pruning (Scott et al., 2007; Corona et al., 2015) and low thinning (Agee and Skinner, 2005; Crecente-Campo et al., 2009). Low thinning will contribute to reduce the density of ladder fuels and break fuel continuity (García-Llamas et al., 2020). Alternatively, stand thinning could improve the Scots pine self-pruning mechanism of dead branches at the canopy base due to an increased incidence of wind and solar radiation (Mäkinen and Colin, 1999). The implementation of 25th percentile return height LiDAR metric could be generalizable to other Mediterranean conifer forests of Europe and North America where base height and continuity of the forest canopy play a key role in active crown fire incidence (Agee and Skinner, 2005; Safford et al., 2012; García-Llamas et al., 2020). Likewise, low stand thinning, together with low to moderate intensity prescribed fires, could be suitable treatments in Mediterranean young Pyrenean oak stands for reducing the canopy horizontal continuity and the accumulation of surface fuels (Brose et al., 2013), since high canopy density was the main driver of high burn severity. This strategy will preserve the oak trees in the stand with the largest diameter, which are the most fire-resistant because of the thicker bark and tall crown (Agee and Skinner, 2005; Fernandes et al., 2010; Corona et al., 2015). In general, thinning treatments in conifer and broadleaf ecosystems should maintain enough canopy closure to limit understory fuel development (Viedma et al., 2020). In heath ecosystems dominated by *Erica australis*, as in other Mediterranean ecosystems such as chaparral and gorse shrublands, prescribed fire could be one of the most effective pre-fire management actions to reduce fuel load (Ascoli and Bovio, 2010; Fernandes, 2015) and increase landscape heterogeneity by creating stand age mosaics (Keeley, 2002). Based on the results of this work, the development of a diverse heathland structure is essential for reducing the risk of stand replacing fires (Harper et al., 2018). In fact, this treatment should be effective in areas with little vegetation three-dimensional heterogeneity identified by low LiDAR rumple index values, particularly on warmer aspects with low fuel moisture content. Prescribed fire might be also a target action on the breakdown of fuel horizontal continuity in gorse and broom ecosystems with a high canopy cover (Fernandes, 2015; Lasanta et al., 2018).

## 5. Conclusions

In the heterogeneous landscapes of the western Mediterranean Basin, burn severity relies largely on forest fuel composition, structure and connectedness. The present study is pioneer in evaluating the potential of airborne LiDAR and bLSA data fusion for estimating pre-fire vegetation features related to high wildfire damage across different fire-prone ecosystems. The results of this study indicate that severe ecosystem damage is mainly driven by vegetation structure rather than topography or patch size, with different roles of pre-fire fuel structure parameters across the target ecosystems. In forest ecosystems, LiDAR metrics overwhelm the contribution of bLSA to explain burn severity spatial patterns. Specifically, closed canopies with high horizontal fuel continuity promote high burn severities in young Pyrenean oak stands. In Scots pine ecosystems, burn severity can be accurately predicted by the vertical distribution of fuel load, being low canopy base height strongly associated with increased burn severity. LiDAR data also gain special relevance in heath shrub ecosystems, where a high horizontal and vertical fuel connectedness increase the likelihood of severe fire effects. Conversely, bLSA products outperform LiDAR metrics to estimate fuel structure and predict burn severity patterns in shrub ecosystems characterized by sparse vegetation cover, such as those dominated by gorse and broom species. In these ecosystems, high aboveground biomass estimated through bLSA is strongly related with high burn severity. Presumably, LiDAR data with a higher pulse density could have improved the contribution of vertical structure metrics in ecosystems dominated by low-growing vegetation. Furthermore, emergent technologies, such as airborne multispectral LiDAR sensors, should be investigated further for the assessment of burn severity fuel drivers. Future research should also consider fire weather and fire propagation at ecosystem level, as they may exert dominant control over burn severity in relation to topography under extreme climatic conditions. The results of this study evidenced that LiDAR and bLSA data fusion is an especially valuable remote sensing tool for the identification of priority areas in fire-prone landscapes where implement pre-fire fuel management strategies aimed to reduce the most adverse ecological effects of severe wildfires. Silviculture actions should be oriented to promote a limited horizontal and vertical fuel continuity considering vegetation characteristics. The proposed methodology might be extrapolated to other Mediterranean ecosystems with similar structure and function in order to reduce uncertainties related to wildfire management.

## Credit author statement

**José Manuel Fernández-Guisuraga:** Conceptualization, Methodology, Validation, Formal analysis, Investigation, Writing - Original Draft. **Susana Suárez-Seoane:** Conceptualization, Methodology, Investigation, Resources, Writing - Review & Editing, Project administration, Funding acquisition. **Paula García-Llamas:** Methodology, Formal analysis, Investigation, Writing - Review & Editing.

**Leonor Calvo:** Conceptualization, Methodology, Investigation, Resources, Writing - Review & Editing, Project administration, Funding acquisition.

## Uncited reference

.

## Declaration of competing interest

The authors declare that they have no known competing financial interests or personal relationships that could have appeared to influence the work reported in this paper.

## Acknowledgements

This study was financially supported by the Spanish Ministry of Economy and Competitiveness, and the European Regional Development Fund (ERDF), in the framework of the GESFIRE (AGL2013-48189-C2-1-R) and FIRESEVES (AGL2017-86075-C2-1-R) projects; and by the Regional Government of Castilla and León in the framework of the FIRECYL (LE033U14), SEFIRECYL (LE001P17) and WUIFIRECYL (LE005P20) projects. J.M. Fernández-Guisuraga is supported by a predoctoral fellowship from the Spanish Ministry of Education (FPU16/03070).

## References

Agee, J.K., Bahro, B., Finney, M.A., Omi, P.N., Sapsis, D.B., Skinner, C.N., van Wagtendonk, J.W., Weatherspoon, C.P., 2000. The use of shaded fuelbreaks in landscape fire management. For. Ecol. Manag. 127, 55–66.

Agee, J.K., Skinner, C.N., 2005. Basic principles of forest fuel reduction treatments. For. Ecol. Manag. 211, 83–96.

Alexander, J.D., Seavy, N.E., Ralph, C.J., Hogoboom, B., 2006. Vegetation and topographical correlates of fire severity from two fires in the Klamath-Siskiyou region of Oregon and California. Int. J. Wildland Fire 15, 237–245.

Andersen, H.E., McGaughey, R.J., Reutebuch, S.E., 2005. Estimating forest canopy fuel parameters using LIDAR data. Rem. Sens. Environ. 94, 441–449.

Archibald, S., Lehmann, C.E.R., Belcher, C.M., Bond, W.J., Bradstock, R.A., Daniau, A.L., Dexter, K.G., Forrestel, E.J., Greve, M., He, T., Higgins, S.I., Hoffmann, W.A., Lamont, B.B., McGlinn, D.J., Moncrieff, G.R., Osborne, C.P., Pausas, J.G., Price, O., Ripley, B.S., Rogers, B.M., Schwilk, D.W., Simon, M.F., Turetsky, M.R., Van der Werf, G.R., Zanne, A.E., 2018. Biological and geophysical feedbacks with fire in the Earth system. Environ. Res. Lett. 13, 033003.

Ascoli, D., Bovio, G., 2010. Appraising fuel and fire behaviour for prescribed burning application in heathlands of Northwest Italy. In: Proceedings of the VI International Conference on Forest Fire Research, Coimbra, Portugal.

Baeza, J., Raventos, J., Escarré, A., Vallejo, R., 2006. Fire risk and vegetation structural dynamics in Mediterranean shrubland. Plant Ecol. 187, 189–201.

Barbati, A., Marchetti, M., Chirici, G., Corona, P., 2014. European Forest Types and Forest Europe SFM indicators: tools for monitoring progress on forest biodiversity conservation. For. Ecol. Manag. 321, 145–157.

Bassett, M., Leonard, S.W.J., Chia, E.K., Clarke, M.F., Bennett, A.F., 2017. Interacting effects of fire severity, time since fire and topography on vegetation structure after wildfire. For. Ecol. Manag. 396, 26–34.

Bennett, L.T., Bruce, M.J., MacHunter, J., Kohout, M., Tanase, M.A., Aponte, C., 2016. Mortality and recruitment of fire-tolerant eucalypts as influenced by wildfire severity and recent prescribed fire. For. Ecol. Manag. 380, 107–117.

Bradstock, R.A., Gill, A.M., Williams, R.J., 2002. Flammable Australia: the Fire Regimes and Biodiversity of a Continent. first ed. Cambridge University Press, Cambridge.

Broncano, M.J., Retana, J., 2004. Topography and forest composition affecting the variability in fire severity and postfire regeneration occurring after a large fire in the Mediterranean basin. Int. J. Wildland Fire 13, 209–216.

Brose, P.H., Dey, D.C., Waldrop, T.A., 2013. The Fire–Oak Literature of Eastern North America: Synthesis and Guidelines General Technical Report NRS-135 USDA Forest Service, Northern Research Station, Irvine, United states.

Burai, P., Deák, B., Valkó, O., Tomor, T., 2015. Classification of herbaceous vegetation using airborne hyperspectral imagery. Rem. Sens. 7, 2046–2066.

Catry, F.X., Rego, F., Moreira, F., Fernandes, P.M., Pausas, J.G., 2010. Post-fire tree mortality in mixed forests of central Portugal. For. Ecol. Manag. 260, 1184–1192.

Chirici, G., Scotti, R., Montaghi, A., Barbati, A., Cartisano, R., Lopez, G., Marchetti, M., McRoberts, R.E., Olsson, H., Corona, P., 2013. Stochastic gradient boosting classification trees for forest fuel types mapping through airborne laser scanning and IRS LISS-III imagery. Int. J. Appl. Earth Obs. Geoinf. 25, 87–97.

R.H.B. Christensen Cumulative link models for ordinal regression with the R package ordinal https://cran.r-project.org/web/packages/ordinal/vignettes/clm_article.pdf 2018 s1 December 2019

R.H.B. Christensen Ordinal - regression models for ordinal data. R package version 2019.4-25 http://www.cran.r-project.org/package=ordinal/ 2019

Chuvieco, E., Aguado, I., Yebra, M., Nieto, H., Salas, J., Martín, M.P., Vilar, L., Martínez, J., Martín, S., Ibarra, P., de la Riva, J., Baeza, J., Rodríguez, F., Molina, J.R., Herrera, M.A., Zamora, R., 2010. Development of a framework for fire risk assessment using remote sensing and geographic information system technologies. Ecol. Model. 221 (1), 46–58.

CNIG Centro de descargas del Centro Nacional de Información Geográfica http://centrodedescargas.cnig.es/CentroDescargas/index.jsp/ 2020 s13 March 2020

Copernicus Open Access Hub, 2020. https://scihub.copernicus.eu/(accessed 01 March 2020).

Coppoletta, M., Merriam, K., Collins, B., 2016. Post-fire vegetation and fuel development influences fire severity patterns in reburns. Ecol. Appl. 26, 686–699.

Corona, P., Ascoli, D., Barbati, A., Bovio, G., Colangelo, G., Elia, M., Garfì, V., Iovino, F., Lafortezza, R., Leone, V., Lovreglio, R., Marchetti, M., Marchi, E., Menguzzato, G., Nocentini, S., Picchio, R., Portoghesi, L., Puletti, N., Sanesi, G., Chianucci, F., 2015. Integrated forest management to prevent wildfires under Mediterranean environments. Annals of Silvicultural Research 39, 1–22.

Costa, P., Castellnou, M., Larranaga, A., Miralles, M., Kraus, D., 2011. Prevention of Large Wildfires Using the Fire Types Concept. Fire Paradox European Project, Generalitat de Catalunya.

Crecente-Campo, F., Pommerening, A., Rodríguez-Soalleiro, R., 2009. Impacts of thinning on structure, growth and risk of crown fire in a Pinus sylvestris L. plantation in northern Spain. For. Ecol. Manag. 257, 1945–1954.

Dillon, G.K., Holden, Z.A., Morgan, P., Crimmins, M.A., Heyerdahl, E.K., Luce, C.H., 2011. Both topography and climate affected forest and woodland burn severity in two regions of the western US, 1984 to 2006. Ecosphere 2, 1–33.

Dunn, C.J., Bailey, J.D., 2016. Tree mortality and structural change following mixed-severity fire in Pseudotsuga forests of Oregon's western Cascades, USA. For. Ecol. Manag. 365, 107–118.

Eskelson, B.N.I., Temesgen, H., Hagar, J.C., 2012. A comparison of selected parametric and imputation methods for estimating snag density and snag quality attributes. For. Ecol. Manag. 272, 26–34.

Estes, B.L., Knapp, E.E., Skinner, C.N., Miller, J.D., Preisler, H.K., 2017. Factors influencing fire severity under moderate burning conditions in the Klamath Mountains, northern California USA. Ecosphere 8, e01794.

Fang, L., Yang, J., White, M., Liu, Z., 2018. Predicting potential fire severity using vegetation, topography and surface moisture availability in a eurasian boreal forest landscape. Forests 9, 130.

Fernandes, P., Luz, A., Loureiro, C., 2010. Changes in wildfire severity from maritime pine woodland to contiguous forest types in the mountains of northwestern Portugal. For. Ecol. Manag. 260, 883–892.

Fernandes, P.M., 2013. Fire-smart management of forest landscapes in the Mediterranean basin under global change. Landsc. Urban Plann. 110, 175–182.

Fernandes, P.M., 2015. Empirical support for the use of prescribed burning as a fuel treatment. Current Forestry Reports 1, 118–127.

Fernandes, P.M., Barros, A.M.G., Pinto, A., Santos, J.A., 2016. Characteristics and controls of extremely large wildfires in the western Mediterranean Basin. J. Geophys. Res.: Biogeosciences 121, 2141–2157.

Fernández-Alonso, J.M., Vega, J.A., Jiménez, E., Ruiz-González, A.D., Álvarez-González, J.G., 2017. Spatially modeling wildland fire severity in pine forests of Galicia, Spain. Eur. J. For. Res. 136, 105–121.

Fernández-García, V., Santamarta, M., Fernández-Manso, A., Quintano, C., Marcos, E., Calvo, L., 2018. Burn severity metrics in fire-prone pine ecosystems along a climatic gradient using Landsat imagery. Rem. Sens. Environ. 206, 205–217.

Fernández-Guisuraga, J.M., Verrelst, J., Calvo, L., Suárez-Seoane, S., 2021. Hybrid inversion of radiative transfer models based on high spatial resolution satellite reflectance data improves fractional vegetation cover retrieval in heterogeneous ecological systems after fire. Rem. Sens. Environ. 255, 112304.

Fernandez-Manso, A., Quintano, C., Roberts, D.A., 2019. Burn severity analysis in Mediterranean forests using maximum entropy model trained with EO-1 Hyperion and LiDAR data. ISPRS J. Photogrammetry Remote Sens. 155, 102–118.

Flatley, W.T., Lafon, C.W., Grissino-Mayer, H.D., 2011. Climatic and topographic controls on patterns of fire in the southern and central Appalachian Mountains, USA. Landsc. Ecol. 26, 195–209.

Fox, J., Hong, J., 2009. Effect displays in R for multinomial and proportional-odds logit models: extensions to the effects package. J. Stat. Software 32, 1–24.

Fox, J., Weisberg, S., 2019. An R Companion to Applied Regression. third ed. (Thousand Oaks, United States).

García-Llamas, P., Suárez-Seoane, S., Taboada, A., Fernández-Manso, A., Quintano, C., Fernández-García, V., Fernández-Guisuraga, J.M., Marcos, E., Calvo, L., 2019a. Environmental drivers of fire severity in extreme fire events that affect Mediterranean pine forest ecosystems. For. Ecol. Manag. 433, 24–32.

García-Llamas, P., Suárez-Seoane, S., Fernández-Guisuraga, J.M., Fernández-García, V., Fernández-Manso, A., Quintano, C., Taboada, A., Marcos, E., Calvo, L., 2019b. Evaluation and comparison of Landsat 8, Sentinel-2 and Deimos-1 remote sensing indices for assessing burn severity in Mediterranean fire-prone ecosystems. Int. J. Appl. Earth Obs. Geoinf. 80, 137–144.

García-Llamas, P., Suárez-Seoane, S., Taboada, A., Fernández-García, V., Fernández-Guisuraga, J.M., Fernández-Manso, A., Quintano, C., Marcos, E., Calvo, L., 2019c. Assessment of the influence of biophysical properties related to fuel conditions on fire severity using remote sensing techniques: a case study on a large fire in NW Spain. Int. J. Wildland Fire 28, 512–520.
García-Llamas, P., Suárez-Seoane, S., Fernández-Manso, A., Quintano, C., Calvo, L., 2020. Evaluation of fire severity in fire prone-ecosystems of Spain under two different environmental conditions. J. Environ. Manag. 271, 110706.
GEODE Mapa geológico digital continuo de España http://mapas.igme.es/gis/services/Cartografia_Geologica/IGME_Geode_50/MapServer/WMSServer/ 2019 s22 November 2019
González, J.R., Pukkala, T., 2007. Characterization of forest fires in Catalonia (north-east Spain). Eur. J. For. Res. 126, 421–429.
Guisan, A., Harrell, F.E., 2000. Ordinal response regression models in ecology. J. Veg. Sci. 11, 617–626.
Harper, A.R., Doerr, S.H., Santin, C., Froyd, C.A., Sinnadurai, P., 2018. Prescribed fire and its impacts on ecosystem services in the UK. Sci. Total Environ. 624, 691–703.
Harrell, F.E., 2019. Rms: Regression Modeling Strategies. R Package Version 5.1. 3.1 https://CRAN.R-project.org/package=rms.
Harris, L., Taylor, A.H., 2017. Previous burns and topography limit and reinforce fire severity in a large wildfire. Ecosphere 8, e02019.
Huy, B., Tinh, N.T., Poudel, K.P., Frank, B.M., Temesgen, H., 2019. Taxon-specific modeling systems for improving reliability of tree aboveground biomass and its components estimates in tropical dry dipterocarp forests. For. Ecol. Manag. 437, 156–174.
ITACyL Proyecto SUELOS http://ftp.itacyl.es/Edafologia/ 2019 s22 November 2019
Jakubowski, M.K., Guo, Q., Kelly, M., 2013. Tradeoffs between lidar pulse density and forest measurement accuracy. Rem. Sens. Environ. 130, 245–253.
Kane, V.R., Gillespie, A.R., McGaughey, R., Lutz, J.A., Ceder, K., Franklin, J.F., 2008. Interpretation and topographic compensation of conifer canopy self-shadowing. Rem. Sens. Environ. 112, 3820–3832.
Kane, V.R., McGaughey, R.J., Bakker, J.D., Gersonde, R.F., Lutz, J.A., Franklin, J. F., 2010. Comparisons between field- and LiDAR-based measures of stand structural complexity. Can. J. For. Res. 40, 761–773.
Kane, V.R., Lutz, J.A., Roberts, S.L., Smith, D.F., McGaughey, R.J., Povak, N.A., Brooks, M.L., 2013. Landscape-scale effects of fire severity on mixed-conifer and red fir forest structure in Yosemite national park. For. Ecol. Manag. 287, 17–31.
Kane, V.R., Lutz, J.A., Cansler, C.A., Povak, N.A., Churchill, D.J., Smith, D.F., Kane, J.T., North, M.P., 2015a. Water balance and topography predict fire and forest structure patterns. For. Ecol. Manag. 338, 1–13.
Kane, V.R., Cansler, C.A., Povak, N.A., Kane, J.T., McGaughey, R.J., Lutz, J.A., Churchill, D.J., North, M.P., 2015b. Mixed severity fire effects within the Rim fire: relative importance of local climate, fire weather, topography, and forest structure. For. Ecol. Manag. 358, 62–79.
Keeley, J., 2002. Fire management of California shrubland landscapes. Environ. Manag. 29, 395–408.
Keeley, J.E., 2009. Fire intensity, fire severity and burn severity: a brief review and suggested usage. Int. J. Wildland Fire 18, 116–126.
Kelly, M., Su, Y., Di Tommaso, S., Fry, D.L., Collins, B.M., Stephens, S.L., Guo, Q., 2018. Impact of error in lidar-derived canopy height and canopy base height on modeled wildfire behavior in the Sierra Nevada, California, USA. Rem. Sens. 10, 10.
Key, C.H., Benson, N.C., 2006. Landscape assessment (LA). In: Lutes, D.C., Keane, R.E., Caratti, J.F., Key, C.H., Benson, N.C., Sutherland, S., Gangi, L.J. (Eds.), FIREMON: Fire Effects Monitoring and Inventory System. Gen. Tech. Rep. RMRS-GTR-164-CD. Department of Agriculture, Forest Service, Rocky Mountain Research Station, Fort Collins, United States, pp. 1–55.
Koetz, B., Morsdorf, F., van der Linden, S., Curt, T., Allgöwer, B., 2008. Multi-source land cover classification for forest fire management based on imaging spectrometry and LiDAR data. For. Ecol. Manag. 256, 263–271.
Kuusinen, N., Stenberg, P., Korhonen, L., Rautiainen, M., Tomppo, E., 2016. Structural factors driving boreal forest albedo in Finland. Rem. Sens. Environ. 175, 43–51.
Kwak, D.A., Cui, G., Lee, W.K., Cho, H.K., Jeon, S.W., Lee, S.H., 2014. Estimating plot volume using lidar height and intensity distributional parameters. Int. J. Rem. Sens. 35, 4601–4629.
Lasanta, T., Khorchani, M., Pérez-Cabello, F., Errea, P., Sáenz-Blanco, R., Nadal-Romero, E., 2018. Clearing shrubland and extensive livestock farming: active prevention to control wildfires in the Mediterranean mountains. J. Environ. Manag. 227, 256–266.
Lasslop, G., Coppola, A.I., Voulgarakis, A., Yue, C., Veraverbeke, S., 2019. Influence of fire on the carbon cycle and climate. Current Climate Change Reports 5, 112–123.
Lecina-Diaz, J., Alvarez, A., Retana, J., 2014. Extreme fire severity patterns in topographic, convective and wind-driven historical wildfires of mediterranean pine forests. PloS One 9, e85127.
Lee, S.W., Lee, M.B., Lee, Y.G., Won, M.S., Kim, J.J., Hong, S.K., 2009. Relationship between landscape structure and burn severity at the landscape and class levels in Samchuck, South Korea. For. Ecol. Manag. 258, 1594–1604.
Li, Z., Erb, A., Sun, Q., Liu, Y., Shuai, Y., Wang, Z., Boucher, P., Schaaf, C., 2018. Preliminary assessment of 20-m surface albedo retrievals from sentinel-2A surface reflectance and MODIS/VIIRS surface anisotropy measures. Rem. Sens. Environ. 217, 352–365.
Liang, S., 2001. Narrowband to broadband conversions of land surface albedo I: Algorithms. Rem. Sens. Environ. 76, 213–238.
Liang, S., Li, X., Wang, J., 2012. Advanced Remote Sensing. second ed. Academic Press, Cambridge, United States.
Lukeš, P., Stenberg, P., Rautiainen, M., 2013. Relationship between forest density and albedo in the boreal zone. Ecol. Model. 261–262, 74–79.
Lydersen, J., North, M., 2012. Topographic variation in structure of mixed-conifer forests under an active-fire regime. Ecosystems 15, 1134–1146.
Maingi, J.K., Henry, M.C., 2007. Factors influencing wildfire occurrence and distribution in eastern Kentucky, USA. Int. J. Wildland Fire 16, 23–33.
Mäkinen, H., Colin, F., 1999. Predicting the number, death, and self-pruning of branches in Scots pine. Can. J. For. Res. 29, 1225–1236.
Mäkinen, H., Song, T., 2002. Evaluation of models for branch characteristics of Scots pine in Finland. For. Ecol. Manag. 158, 25–39.
McCune, B., Keon, D., 2002. Equations for potential annual direct incident radiation and heat load. J. Veg. Sci. 13, 603–606.
McGaughey, R.J., 2018. FUSION/LDV: Software for LiDAR Data Analysis and Visualization. version 3.80.
Miller, J.D., Thode, A.E., 2007. Quantifying burn severity in a heterogeneous landscape with a relative version of the delta normalized burn ratio (dNBR). Rem. Sens. Environ. 109, 66–80.
Mitsopoulos, I.D., Dimitrakopoulos, A.P., 2007. Canopy fuel characteristics and potential crown fire behavior in Aleppo pine (Pinus halepensis Mill.) forests. Ann. For. Sci. 64, 287–299.
Mitsopoulos, I., Chrysafi, I., Bountis, D., Mallinis, G., 2019. Assessment of factors driving high fire severity potential and classification in a Mediterranean pine ecosystem. J. Environ. Manag. 235, 266–275.
Mon, M.S., Mizoue, N., Htun, N.Z., Kajisa, T., Yoshida, S., 2012. Factors affecting deforestation and forest degradation in selectively logged production forest: a case study in Myanmar. For. Ecol. Manag. 267, 190–198.
Montealegre, A.L., Lamelas, M.T., Tanase, M.A., de la Riva, J., 2014. Forest fire severity assessment using ALS data in a mediterranean environment. Rem. Sens. 6, 4240–4265.
Morsy, S., Shaker, A., El-Rabbany, A., 2017. Multispectral LiDAR data for land cover classification of urban areas. Sensors 17, 958.
Naegeli, K., Damm, A., Huss, M., Wulf, H., Schaepman, M., Hoelzle, M., 2017. Cross-Comparison of albedo products for glacier surfaces derived from airborne and satellite (Sentinel-2 and Landsat 8) optical data. Rem. Sens. 9, 110.
Nagelkerke, N.J.D., 1991. A note on a general definition of the coefficient of determination. Biometrika 78, 691–692.
Niccoli, F., Esposito, A., Altieri, S., Giovanna, B., 2019. Fire severity influences ecophysiological responses of Pinus pinaster ait. Front. Plant Sci. 10, 539.
Ninyerola, M., Pons, X., Roure, J.M., 2005. Atlas Climático Digital de la Península Ibérica. Metodología y aplicaciones en bioclimatología y geobotánica. Universidad Autónoma de Barcelona.
Oliveras, I., Gracia, M., Gerard, M., Retana, J., 2009. Factors influencing the pattern of fire severities in a large wildfire under extreme meteorological conditions in the Mediterranean basin. Int. J. Wildland Fire 18, 755–764.
Parks, S.A., Holsinger, L.M., Panunto, M.H., Jolly, W.M., Dobrowski, S.Z., Dillon, G.K., 2018. High-severity fire: evaluating its key drivers and mapping its probability across western US forests. Environ. Res. Lett. 13, 044037.
Paula, S., Ojeda, F., 2006. Resistance of three co-occurring resprouter Erica species to highly frequent disturbance. Plant Ecol. 183, 329–336.
Pausas, J.G., Keeley, J.E., 2009. A burning story: the role of fire in the history of life. Bioscience 59, 593–601.
Perchemlides, K.A., Muir, P.S., Hosten, P.E., 2008. Responses of chaparral and oak woodland plant communities to fuel-reduction thinning in southwestern Oregon. Rangel. Ecol. Manag. 61, 98–109.
Plucinski, M.P., 2003. The Investigation of Factors Governing Ignition and Development of Fires in Heathland Vegetation Thesis dissertation The University of New South Wales, Sidney, Australia.
Pnoa Plan Nacional de Observación del Territorio https://pnoa.ign.es/ 2020 s13 March 2020
Quintano, C., Fernández-Manso, A., Calvo, L., Roberts, D.A., 2019. Vegetation and soil fire damage analysis based on species distribution modeling trained with multispectral satellite data. Rem. Sens. 11, 1832.
R Core Team, 2019. R: A Language and Environment for Statistical Computing. R Foundation for Statistical Computing, Vienna, Austria. https://www.R-project.org/.
Radoux, J., Lamarche, C., Van Bogaert, E., Bontemps, S., Brockmann, C., Defourny, P., 2014. Automated training sample extraction for global land cover mapping. Rem. Sens. 6, 3965–3987.
Richter, R., Schläpfer, D., 2018. Atmospheric/Topographic Correction for Satellite Imagery. DLR Report DLR-IB 565-01/2018, Wessling, Germany.
Rivas-Martínez, S., Rivas-Sáenz, S., Penas, A., 2011. Worldwide bioclimatic classification system. Global Geobotany 1, 1–634 + 4 Maps.
Roberts, D.W., Cooper, S.V., 1989. Concepts and techniques of vegetation mapping. In: Ferguson, D.E., Morgan, P., Johnson, F.D. (Eds.), Land Classifications Based on Vegetation: Applications for Resource Management. USDA Forest Service, Moscow, United States, pp. 90–96.
Robinne, F.N., Hallema, D.W., Bladon, K.D., Buttle, J.M., 2020. Wildfire impacts on hydrologic ecosystem services in North American high-latitude forests: a scoping review. J. Hydrol. 581, 124360.
Rodríguez-Caballero, E., Knerr, T., Weber, B., 2015. Importance of biocrusts in dryland monitoring using spectral indices. Rem. Sens. Environ. 170, 32–39.

Safford, H.D., Schmidt, D.A., Carlson, C.H., 2009. Effects of fuel treatments on fire severity in an area of wildland–urban interface, Angora Fire, Lake Tahoe Basin, California. For. Ecol. Manag. 258, 773–787.
Safford, H.D., Stevens, J.T., Merriam, K., Meyer, M.D., Latimer, A.M., 2012. Fuel treatment effectiveness in California yellow pine and mixed conifer forests. For. Ecol. Manag. 274, 17–28.
Scott, J.H., Reinhardt, E.D., 2007. Effects of Alternative Treatments on Canopy Fuel Characteristics in Five Conifer Stands General Technical Report PSW-GTR-203 USDA Forest Service, Pacific Southwest Research Station, Albany, United States.
Steel, Z.L., Safford, H.D., Viers, J.H., 2015. The fire frequency-severity relationship and the legacy of fire suppression in California forests. Ecosphere 6, 1–23.
Stephens, S.L., Agee, J.K., Fulé, P.Z., North, M.P., Romme, W.H., Swetnam, T.W., Turner, M.G., 2013. Managing forests and fire in changing climates. Science 342, 41–42.
Strahler, A.H., 1980. The use of prior probabilities in maximum likelihood classification of remotely sensed data. Rem. Sens. Environ. 10, 135–163.
Tian, L., Zhang, Y., Zhu, J., 2014. Decreased surface albedo driven by denser vegetation on the Tibetan Plateau. Environ. Res. Lett. 9, 104001.
Thompson, J.R., Spies, T.A., 2009. Vegetation and weather explain variation in crown damage within a large mixed-severity wildfire. For. Ecol. Manag. 258, 1684–1694.
Turner, M.G., Romme, W.H., 1994. Landscape dynamics in crown fire ecosystems. Landsc. Ecol. 9, 59–77.
Turner, M.G., Romme, W.H., Gardner, R.H., 1999. Prefire heterogeneity, fire severity, and Early Postfire plant reestablishment in subalpine forests of Yellowstone National Park, Wyoming. Int. J. Wildland Fire 9, 21–36.
Vega, J.A., 2007. Empirical Approach to Fire Spread Prediction in Shrublands. Workshop on Mathematical Modeling and Numerical Simulation of Forest Fire Propagation. (Vigo, Spain).
Vanino, S., Nino, P., De Michele, C., Bolognesi, S.F., D'Urso, G., Di Bene, C., Pennelli, B., Vuolo, F., Farina, R., Pulighe, G., Napoli, R., 2018. Capability of Sentinel-2 data for estimating maximum evapotranspiration and irrigation requirements for tomato crop in Central Italy. Rem. Sens. Environ. 215, 452–470.
Venables, W.N., Ripley, B.D., 2002. Modern Applied Statistics with S. fourth ed. Springer, New York, United States.
Viedma, O., Quesada, J., Torres, I., De Santis, A., Moreno, J.M., 2015. Fire severity in a large fire in a Pinus pinaster forest is highly predictable from burning conditions, stand structure, and topography. Ecosystems 18, 237–250.
Viedma, O., Chico, F., Fernández, J.J., Madrigal, C., Safford, H.D., Moreno, J.M., 2020. Disentangling the role of prefire vegetation vs. burning conditions on fire severity in a large forest fire in SE Spain. Rem. Sens. Environ. 247, 111891.
Vilà-Cabrera, A., Coll, L., Martínez-Vilalta, J., Retana, J., 2018. Forest management for adaptation to climate change in the Mediterranean basin: a synthesis of evidence. For. Ecol. Manag. 407, 16–22.
Volpi, V., Tuia, D., Bovolo, F., Kanevski, M., Bruzzone, L., 2013. Supervised change detection in VHR images using contextual information and support vector machines. Int. J. Appl. Earth Obs. Geoinf. 20, 77–85.
Walker, S.H., Duncan, D.B., 1967. Estimation of the probability of an event as a function of several independent variables. Biometrika 54, 167–179.
Wallace, A., Nichol, C., Woodhouse, I., 2012. Recovery of forest canopy parameters by inversion of multispectral LiDAR data. Rem. Sens. 4, 509–531.
Wang, L., Sousa, W.P., Gong, P., Biging, G.S., 2004. Comparison of IKONOS and QuickBird images for mapping mangrove species on the Caribbean coast of Panama. Rem. Sens. Environ. 91, 432–440.
Ward, D.S., Kloster, S., Mahowald, N.M., Rogers, B.M., Randerson, J.T., Hess, P.G., 2012. The changing radiative forcing of fires: global model estimates for past, present and future. Atmos. Chem. Phys. 12, 10857–10886.
Wulder, M.A., White, J.C., Alvarez, F., Han, T., Rogan, J., Hawkes, B., 2009. Characterizing boreal forest wildfire with multi-temporal Landsat and LIDAR data. Rem. Sens. Environ. 113, 1540–1555.
Yang, H., Zhang, X., Xu, M., Shao, S., Wang, X., Liu, W., Wu, D., Ma, Y., Bao, Y., Zhang, X., Liu, H., 2020. Hyper-temporal remote sensing data in bare soil period and terrain attributes for digital soil mapping in the Black soil regions of China. Catena 184, 104259.
Zald, H.S.J., Dunn, C.J., 2018. Severe fire weather and intensive forest management increase fire severity in a multi-ownership landscape. Ecol. Appl. 28, 1068–1080.
Zhang, X., Liao, C., Li, J., Sun, Q., 2013. Fractional vegetation cover estimation in arid and semi-arid environments using HJ-1 satellite hyperspectral data. Int. J. Appl. Earth Obs. Geoinf. 21, 506–512.
Zhao, Y., Wang, X., Novillo, C.J., Arrogante-Funes, P., Vázquez-Jiménez, R., Maestre, F.T., 2018. Albedo estimated from remote sensing correlates with ecosystem multifunctionality in global drylands. J. Arid Environ. 157, 116–123.